A review of extended/generalized finite element methods for material modeling

TOPICAL REVIEW

A review of extended/generalized finite element methods for material modeling

Ted Belytschko[1,3]**, Robert Gracie**[1,4] **and Giulio Ventura**[2,5]

[1] Department of Mechanical Engineering, Northwestern University, 2145 Sheridan Road, Evanston, IL 60208, USA
[2] Department of Structural Engineering and Geotechnics, Politecnico di Torino, 10129 Torino, Italy

E-mail: tedbelytschko@northwestern.edu, rgracie@northwestern.edu and gventura@polito.it

Abstract

The extended and generalized finite element methods are reviewed with an emphasis on their applications to problems in material science: (1) fracture, (2) dislocations, (3) grain boundaries and (4) phases interfaces. These methods facilitate the modeling of complicated geometries and the evolution of such geometries, particularly when combined with level set methods, as for example in the simulation growing cracks or moving phase interfaces. The state of the art for these problems is described along with the history of developments.

1. Introduction

The extended finite element method (XFEM) and the generalized finite element method (GFEM) are versatile tools for the analysis of problems characterized by discontinuities, singularities, localized deformations and complex geometries. These methods can dramatically simplify the solution of many problems in material modeling, such as

  (i) the propagation of cracks,
 (ii) the evolution of dislocations,
(iii) the modeling of grain boundaries and
(iv) the evolution of phase boundaries.

The advantage of these methods is that the finite element mesh can be completely independent of the morphology of these entities. Two examples are shown in figures 1 and 2. The first is a crack in three dimensions. As can be seen, the crack surface and crack front are

---

[3] Author to whom any correspondence should be addressed.
[4] Current address: Department of Civil and Environmental Engineering, University of Waterloo, 200 University Avenue West, Waterloo, Ontario, Canada N2L3G1.
[5] Visiting scholar, Summer 2008, Department of Mechanical Engineering, Northwestern University, 2145 Sheridan Road, Evanston, IL 60202, USA.
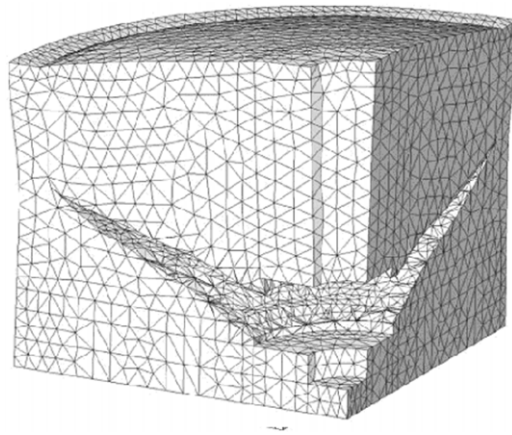
Figure 1. Three-dimensional XFEM model of a crack. Displacements are magnified 200 times [2]. (Reprinted with permission, © Wiley Interscience [2].)
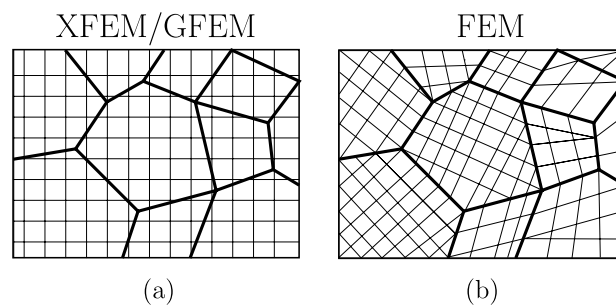

Figure 2. Discretizations of a grain boundary problem for (*a*) an XFEM/GFEM model with a structured (Cartesian) mesh and (*b*) a FEM model.

completely independent of the mesh. This allows for the convenient simulation of the evolution of the cracks because as a crack grows there is no need for remeshing. The second example, shown in figure 2, is a micromodel of a polycrystal. Here the mesh for the XFEM/GFEM model (figure 2(*a*)) is structured and is completely independent of the location of the grain boundaries. In contrast, in the mesh for a standard FEM model, shown in figure 2(*b*), the element edges must conform to the grain boundaries and duplicate nodes must be placed there. The advantages for modeling the complicated grain boundary morphologies which occur in three dimensions can easily be imagined.

Furthermore, when certain aspects of the solution of the field are known, as for example the neartip displacement fields for cracks, enrichment functions based on these fields can be added to the approximation space. For example, for cracks and dislocations in elastic media, the well-known asymptotic singular near-field solutions can be added near crack fronts or dislocation cores as enrichments. This reduces the need for significant *h*-refinement in these subdomains of the problem, especially in two-dimensional models.

The major advantage of these methods for problems in materials science is the simplification of the modeling of discontinuous phenomena. As already mentioned, in conventional finite element methods, the mesh has to be constructed so that element edges/faces coincide with the crack surface and nodes must be placed on each side of the crack to allow

material separation along the crack surface. The construction of such meshes becomes quite difficult, especially in three-dimensional problems, because the mesh also has to account for other features of the model, such as grain boundaries or inclusions. In XFEM, the introduction of a discontinuous displacement field along the crack surface is accomplished by simply introducing additional basis functions into the approximation. Furthermore, as described later, when XFEM is combined with level sets, the entire representation of the feature, such as the geometry and the displacement field of a crack, can be constructed in terms of nodal values at the nodes of the original mesh. Similarly, the modeling of phase boundaries and other discontinuities is facilitated by these methods. These advantages are particularly important when the geometry evolves, as in a growing crack or moving phase boundaries.

The XFEM and GFEM are basically identical methods: the name generalized finite element method (GFEM) was adopted by the Texas school [37, 71, 72] in 1995–1996 and the name extended finite element method (XFEM) was coined by the Northwestern school [10, 75] in 1999. XFEM was developed for discontinuities, such as cracks, and used local enrichments. The first works in GFEM involved global enrichments of the approximation space; however, as early as 2000, local enrichments for singularities at sharp corners were also developed [34].

XFEM/GFEM can be used with both structured and unstructured meshes. Structured meshes are appealing for many studies in materials science, where the objective is to determine the properties of a unit cell of the material. Unstructured meshes, on the other hand, tend to be widely used for the analysis of engineering structures and components since it is often desirable to conform the mesh to the external boundaries of the component, although some methods under development today are able to treat even complicated geometries with structured meshes [15].

This paper is aimed at providing a unified view of the XFEM/GFEM with an emphasis on formulations of interest for materials modeling problems. In addition to summarizing the literature, this paper aims to describe the latest forms of these methods. Therefore, in many cases we will not describe the developments in historical order, but arrange the material according to the problems addressed with the methods described as they are currently used, followed by a summary of the pertinent literature.

The development of XFEM/GFEM was an outgrowth of the extensive research in meshfree methods, Belytschko *et al* [13]. Many of the techniques that are used in XFEM and GFEM are directly related to techniques previously developed in meshfree methods. Therefore we will also point out the relevant literature in meshfree methods. Previous surveys of XFEM have been given by Karihaloo and Xiao [61] and by Abdelaziz and Hamouine [1]; a mathematical survey of XFEM/GFEM was given by Babuska *et al* [6] and a recent review of XFEM for fracture is given by Rabczuk *et al* [85]. A monograph on XFEM focused on fracture has also recently been published [77].

We will start by describing the concept of a partition of unity, which underpins both the XFEM/GFEM. Next, we will discuss the application of XFEM/GFEM to stationary and growing cracks, since these particular applications incorporate most of the features found in many other applications. We will then examine the application of these methods to dislocations, inclusions, phase boundaries and grain boundaries. Subsequently, we will further discuss the application of these methods to cohesive cracks and dynamic fracture and we will discuss some of the implementation issues.

2. Partition of unity enriched finite elements

The foundation of these methods is the partition of unity concept for enriching finite elements or meshfree approximations [37, 71]. A partition of unity in a domain Ω is a set of functions

$\varphi_I(\boldsymbol{x})$ such that

$$\sum_{\forall I} \varphi_I(\boldsymbol{x}) = 1, \qquad \forall \boldsymbol{x} \in \Omega. \tag{1}$$

The property of a partition of unity exploited in XFEM/GFEM is that any function $\Psi(\boldsymbol{x})$ can be reproduced by a product of the partition of unity functions with $\Psi(\boldsymbol{x})$. Furthermore, when the sum is modified by introducing parameters $\boldsymbol{q}_I$, the enrichment function can be adjusted by these parameters by using the approximation

$$\boldsymbol{u}^h(\boldsymbol{x}) = \underbrace{\sum_{\forall I} N_I(\boldsymbol{x})\boldsymbol{u}_I}_{\boldsymbol{u}^{\text{FE}}} + \underbrace{\sum_{\forall I} \varphi_I(\boldsymbol{x})\Psi(\boldsymbol{x})\boldsymbol{q}_I}_{\boldsymbol{u}^{\text{enr}}}, \tag{2}$$

where N_I are the standard FEM shape functions and $\boldsymbol{u}_I$ are the standard nodal degrees of freedom. The first part of the right hand side of (2) is the standard finite element approximation, whereas the second part is the partition of unity enrichment. The nodal values $\boldsymbol{q}_I$ are unknown parameters that adjust the enrichment so that it best approximates the solution at hand ($\Psi(\boldsymbol{x})$ is often based on asymptotic solutions that are not exact solutions). Thus the enrichment need not be precisely the local solution for the problem at hand. Another advantage of this approximation structure is that when the functions $\varphi_I(\boldsymbol{x})$ have compact support (i.e. are only nonzero over a small subdomain of the problem), then the discrete equations for the system will be sparse. By contrast, directly adding an enrichment function to the approximation would lead to nonsparse discrete equations, which are computationally much more expensive.

Note that by the partition of unity property, when $\boldsymbol{q}_I = 1$ and $\boldsymbol{u}_I = 0$, the function $\Psi(\boldsymbol{x})$ is reproduced exactly by the approximation (2). It should be pointed out that the shape functions for the standard approximation and the enrichment need not be the same functions, as indicated in the above, but generally the same functions are used, i.e. generally $\varphi_I(\boldsymbol{x}) = N_I(\boldsymbol{x})$.

All Lagrangian finite element shape functions satisfy the partition of unity property, since this property is essential for convergence and passing the patch test because the partition of unity property enables a finite element approximation to represent rigid body translation exactly. Similarly, many meshfree approximations also satisfy this property.

The introduction of the partition of unity concept to enrich solution spaces of numerical solutions to partial differential equations is usually attributed to Melenk and Babuška [71], where it was called the partition of unity method (PUM). The PUM is the progenitor of both XFEM and GFEM. Some of the applications envisioned in that paper are singularities at corners, boundary layers and improved approximations for the Laplace and Helmholtz equations by a harmonic enrichment. They also give a convergence proof of the method. Earlier, some of the same concepts were proposed by Babuška *et al* [7]. The partition of unity concept was introduced in meshless methods by Duarte and Oden [37].

An even earlier development of the same basic idea can be found in Shi [89] where it was called the manifold method. A more accessible description of the manifold method (now called the finite cover method) can be found in Terada *et al* [103]. This method is closely related to the PUM as is a recent method for cracks developed by Hansbo and Hansbo [53], which is discussed in section 11.

3. Cracks

We begin with a description of the application of XFEM to cracks. Consider a finite element model of a cracked body, as shown in figure 3. Let the set of all nodes in the finite element mesh be denoted by $\mathcal{S}$, the set of nodes of elements around the crack tip (or crack front in

three dimensions) be denoted by $\mathcal{S}_C$ and the set of nodes of elements cut by the crack, i.e. the discontinuity, but not in $\mathcal{S}_C$ be denoted by $\mathcal{S}_H$. The set of elements with nodes in $\mathcal{S}_C$ can be selected by the user. Usually one element, as shown at crack tip B in figure 3, suffices, but some improvements in accuracy can be obtained by using several elements, as shown at crack tip A in figure 3. Nodes in $\mathcal{S}_C$ and $\mathcal{S}_H$ will be referred to as tip enriched and step enriched nodes, respectively, and collectively as enriched nodes.

Let the crack surface be given by an implicit function description, i.e. a level set, $f(\boldsymbol{x}) = 0$ (describing the crack in this manner enables the method to treat discontinuities such as cracks without any supplementary data other than nodal points, as shown later) and let $f(\boldsymbol{x})$ have opposite signs on the two sides of the crack. In most applications, $\varphi_I = N_I$ and we will use this. The XFEM displacement field for a crack is

$$\boldsymbol{u}^h(\boldsymbol{x}) = \sum_{\forall I} N_I(\boldsymbol{x})\boldsymbol{u}_I + \sum_{J \in \mathcal{S}_H} N_J(\boldsymbol{x})[H(f(\boldsymbol{x})) - H(f(\boldsymbol{x}_J))]\boldsymbol{q}_J^0$$

$$+ \sum_j \sum_{K \in \mathcal{S}_C} N_K(\boldsymbol{x})[\Psi^{(j)}(\boldsymbol{x}) - \Psi^{(j)}(\boldsymbol{x}_K)]\boldsymbol{q}_K^{(j)}, \tag{3}$$

where $H(\cdot)$ is the Heaviside step function given by

$$H(f) = \begin{cases} 1, & f > 0 \\ 0, & \text{otherwise} \end{cases} \tag{4}$$

and where $\Psi^{(j)}$ is a set of enrichment functions which approximate the neartip behavior, $\boldsymbol{q}_I^{(j)}$ are the enrichment coefficients which are additional unknowns at the nodes and $\boldsymbol{x}_J$ is the position of node J.

It should be stressed that (3) is a *local partition of unity* in contrast to the global form in (2), i.e. the enrichment is added only where it is useful. This substantially improves the computational efficiency because in general far fewer unknowns are introduced by the enrichment than in a global partition of unity. There are some difficulties in the blending elements around tip enriched elements (indicated by cross-hatching in figure 3 in local partitions of unity methods), but these are now resolved, as discussed in section 9.

It is worthwhile to illustrate how the discontinuity is introduced by this approximation. Since $f(\boldsymbol{x})$ defines the crack and since $f(\boldsymbol{x})$ changes sign along the crack, it follows the $H(f(\boldsymbol{x}))$ is discontinuous along the crack. We can furthermore show that for elements cut by the crack, the jump in the displacement field across the crack Γ_c is

$$[|\boldsymbol{u}^h(\boldsymbol{x})|]_{\Gamma_c} = \sum_{J \in \mathcal{S}_H} N_J(\boldsymbol{x})\boldsymbol{q}_J^0, \qquad \boldsymbol{x} \in \Gamma_c. \tag{5}$$

Thus the magnitude of the crack-opening displacement directly depends on $\boldsymbol{q}_J^0$.

Note that in (3) the enrichment function is shifted so that the product of the shape function N_I and the enrichment function vanish at each node, as proposed in Belytschko *et al* [15]. Consequently, the step function enrichment for the discontinuity vanishes at the edges of all elements not crossed by the discontinuity and $\boldsymbol{u}^h(\boldsymbol{x}_J) = \boldsymbol{u}_J$. Therefore, only those elements that are crossed by the discontinuity need to be treated differently. In addition, this shifting simplifies the blending of enriched elements with standard elements as described later. It is sometimes stated that this shifting enables one to satisfy displacement boundary conditions,
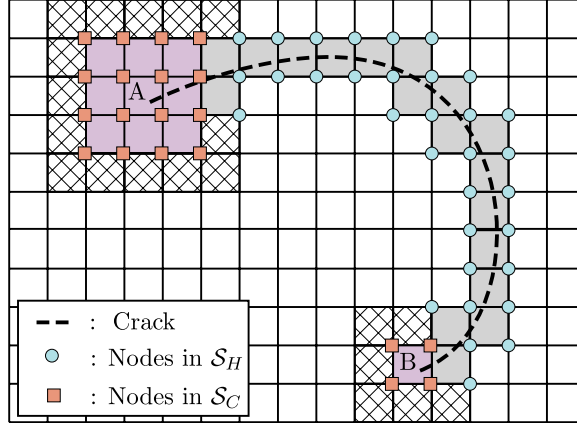
Figure 3. An arbitrary crack line (dashed line) in a structured mesh with step enriched (light gray) and tip enriched (purple) elements. Nodes in sets $\mathcal{S}_C$ and $\mathcal{S}_H$ are denoted by red squares and blue circles, respectively.

just as in the standard finite element method, by setting the nodal displacements appropriately, but this is not strictly true: the displacement boundary conditions will only be met at the nodes when this is done.

For cracks in isotropic elastic materials, the crack tip enrichment functions $\Psi^{(j)}$ are based on the asymptotic solution of Williams [114]. As shown in [44] in the context of meshfree methods, an effective neartip enrichment can be constructed from the following functions

$$\{\Psi_i\}_{i=1}^4 = \sqrt{r}\{\cos(\theta/2), \sin(\theta/2), \sin(\theta/2)\sin(\theta), \cos(\theta/2)\sin(\theta)\}. \qquad (6)$$

Recently, enrichments for orthotropic materials have been given in [4] and a further discussion of their application can be found in [77]. The four enrichment functions for orthotropic materials are only a little more complicated than the functions (6) and are given by

$$\{\Psi_i\}_{i=1}^4 = \sqrt{r}\left\{\cos(\theta_1/2), \cos(\theta_2/2)\sqrt{g_2(\theta)}, \sin(\theta_1/2)\sqrt{g_1(\theta)}, \sin(\theta_2/2)\sqrt{g_2(\theta)}\right\}, \qquad (7)$$

where $g_j(\theta)$ and θ_j are functions and angles defined by relatively simple formulae. Furthermore, they show that these enrichments provide good accuracy for a variety of orthotropic fracture problems.

3.1. Discrete equations

The discrete XFEM equations are obtained by the substitution of (3) into the principle of virtual work. Assuming that the system is linear leads to the following system of discrete equations

$$\begin{bmatrix} \boldsymbol{K}^{uu} & \boldsymbol{K}^{u0} & \cdots & \boldsymbol{K}^{u4} \\ \boldsymbol{K}^{u0\top} & \boldsymbol{K}^{00} & \cdots & \boldsymbol{K}^{04} \\ \vdots & \vdots & \ddots & \vdots \\ \boldsymbol{K}^{u4\top} & \boldsymbol{K}^{14\top} & \cdots & \boldsymbol{K}^{44} \end{bmatrix} \begin{Bmatrix} \boldsymbol{d}^u \\ \boldsymbol{d}^0 \\ \vdots \\ \boldsymbol{d}^4 \end{Bmatrix} = \begin{Bmatrix} \boldsymbol{f}^{\text{ext}} \\ \boldsymbol{Q}^0 \\ \vdots \\ \boldsymbol{Q}^4 \end{Bmatrix}, \qquad (8)$$

where the vector of standard finite element degrees of freedom is $\boldsymbol{d}^u = \{\boldsymbol{u}_1, \ldots, \boldsymbol{u}_n\}^\top$ and the vectors of enriched degrees of freedom are $\boldsymbol{d}^0 = \{\boldsymbol{q}_1^0, \ldots, \boldsymbol{q}_{n_H}^0\}^\top$ and $\boldsymbol{d}^i = \{\boldsymbol{q}_1^i, \ldots, \boldsymbol{q}_{n_C}^i\}^\top$. The

scalars n, n_H and n_C are the number of nodes in $\mathcal{S}$, $\mathcal{S}_H$ and $\mathcal{S}_C$, respectively. The stiffness matrices are given by

$$\boldsymbol{K}_{IJ}^{uu} = \int_{\Omega} \boldsymbol{B}_I \boldsymbol{C} \boldsymbol{B}_J \, d\Omega, \tag{9}$$

$$\boldsymbol{K}_{IJ}^{uj} = \int_{\Omega} \boldsymbol{B}_I \boldsymbol{C} \mathcal{B}_J^{(j)} \, d\Omega, \qquad j \in \{0, 1, 2, 3, 4\}, \tag{10}$$

$$\boldsymbol{K}_{IJ}^{ij} = \int_{\Omega} \mathcal{B}_I^{(i)} \boldsymbol{C} \mathcal{B}_J^{(j)} \, d\Omega, \qquad i, j \in (0, 1, 2, 3, 4), \tag{11}$$

where $\boldsymbol{C}$ is the elasticity matrix and $\boldsymbol{B}_I$ is the standard finite element strain-displacement matrix which in two dimensions is

$$\boldsymbol{B}_I = \begin{bmatrix} N_{I,x} & 0 \\ 0 & N_{I,y} \\ N_{I,y} & N_{I,x} \end{bmatrix}, \qquad \forall I, \tag{12}$$

where a comma denotes differentiation. The enriched strain-displacement matrices associated with the enriched part of the displacement approximation are

$$\mathcal{B}_I^0 = \begin{bmatrix} (N_I H(f(\boldsymbol{x})) - H(f(\boldsymbol{x}_I)))_{,x} & 0 \\ 0 & (N_I H(f(\boldsymbol{x})) - H(f(\boldsymbol{x}_I)))_{,y} \\ (N_I H(f(\boldsymbol{x})) - H(f(\boldsymbol{x}_I)))_{,y} & (N_I H(f(\boldsymbol{x})) - H(f(\boldsymbol{x}_I)))_{,x} \end{bmatrix}, \qquad \forall I \in \mathcal{S}_H \tag{13}$$

and for $j \in \{1, 2, 3, 4\}$

$$\mathcal{B}_I^j = \begin{bmatrix} (N_I \Psi_j(f(\boldsymbol{x})) - \Psi_j(f(\boldsymbol{x}_I)))_{,x} & 0 \\ 0 & (N_I \Psi_j(f(\boldsymbol{x})) - \Psi_j(f(\boldsymbol{x}_I)))_{,y} \\ (N_I \Psi_j(f(\boldsymbol{x})) - \Psi_j(f(\boldsymbol{x}_I)))_{,y} & (N_I \Psi_j(f(\boldsymbol{x})) - \Psi_j(f(\boldsymbol{x}_I)))_{,x} \end{bmatrix}, \qquad \forall I \in \mathcal{S}_C. \tag{14}$$

The Cauchy stress is

$$\boldsymbol{\sigma} = \boldsymbol{C} \left(\sum_{\forall I} \boldsymbol{B}_I \boldsymbol{u}_I + \sum_{J \in \mathcal{S}_H} \mathcal{B}_J^0 \boldsymbol{q}_J^0 + \sum_{K \in \mathcal{S}_C} \sum_{j=1}^{4} \mathcal{B}_K^j \boldsymbol{q}_K^j \right). \tag{15}$$

In the absence of body forces, the force vectors due to external loads are

$$\boldsymbol{f}_I^{\text{ext}} = \int_{\Gamma_t} N_I \bar{\boldsymbol{t}} \, d\Gamma, \qquad \forall I, \tag{16}$$

$$\boldsymbol{Q}_I^0 = \int_{\Gamma_t} N_I (H(f(\boldsymbol{x})) - H(f(\boldsymbol{x}_I))) \bar{\boldsymbol{t}} \, d\Gamma, \qquad I \in \mathcal{S}_H, \tag{17}$$

$$\boldsymbol{Q}_I^j = \int_{\Gamma_t} N_I (\Psi_j(f(\boldsymbol{x})) - \Psi_j(f(\boldsymbol{x}_I))) \bar{\boldsymbol{t}} \, d\Gamma, \qquad I \in \mathcal{S}_C \quad \text{and} \quad j \in \{1, 2, 3, 4\}, \tag{18}$$

where $\bar{\boldsymbol{t}}$ are the applied tractions to the domain boundary Γ_t.

Two important characteristics of the XFEM/GFEM discrete equations are worth noting:

(i) The B-matrices associated with the enriched degrees of freedom (13)–(14) are discontinuous within elements cut by the crack. Therefore the integrands of the stiffness matrices (10)–(11) and the force vectors (17)–(18) are discontinuous. Furthermore, the B-matrix (14) is singular at the crack tip (crack front in three dimensions). So, standard Gauss quadrature is inadequate for evaluating these integrals. Quadrature in XFEM/GFEM is further discussed in section 8.

(ii) The sets $\mathcal{S}_H$ and $\mathcal{S}_C$ are small subsets of the total number of nodes. Therefore, the integrals (10)–(11) and (17)–(18) are only nonzero over a small number of elements.

3.2. Literature review on cracks

The local partition of unity concept was first applied to fracture in Belytschko and Black [10]. The tip enrichment (6) was used for the entire crack, with a mapping to deal with small deviations from a straight crack. In Moës *et al* [75] and Dolbow *et al* [31] the concept of using a Heaviside enrichment in conjunction with a neartip enrichment as described above (3) was introduced along with the name of the method, XFEM. This enables arbitrary curved cracks to be handled with ease independent of the geometry of the mesh. The methodology was extended by Daux *et al* [28] to branched and intersecting cracks by superposing several Heaviside enrichment functions at the junctions.

XFEM was extended to three-dimensional crack problems in Sukumar *et al* [101]. In [101] the same singular enrichment functions as used in two dimensions problems were used (6), but they were expressed in terms of polar coordinates of the plane normal to the crack front. This approach works remarkably well.

Duarte *et al* [35] developed a three-dimensional method for dynamic crack propagation in the GFEM framework with the discontinuity enrichment based on the visibility criterion [63]. They used singular enrichments near the crack front based on the first order term for the asymptotic solutions for straight cracks. Recent improvements and applications in three-dimensional XFEM/GFEM can be found in Areias and Belytschko [2] and Gasser and Holzapfel [47].

Karihaloo and co-workers [68, 115] studied a neartip enrichment basis that includes higher order terms of the asymptotic expansion of the crack tip field in two dimensions. The enrichments are expressed in terms of mode I and mode II stress intensity factors, K_I and K_{II}, so the solution immediately provides these stress intensity factors. This neartip enrichment has proved to be very effective for extracting accurate SIFs in two dimensions; however, applications to three dimensions have not been made.

A study of quadratic elements for brittle fracture has been presented by Stazi *et al* [93], where curved cracks were considered. It was reported that the enrichment $\boldsymbol{u}^{\mathrm{enr}}$ should be constructed with linear shape functions even when the standard FE part of the approximation $\boldsymbol{u}^{\mathrm{FE}}$ is constructed with quadratic shape functions. This result is related to the blending of enriched and unenriched elements and has also been confirmed by Legay *et al* [66] for spectral finite elements.

Legay *et al* [66] studied the modeling of discontinuities in functions and gradients with spectral finite elements. A noteworthy finding was that the difficulties with blending decrease as the order of the element increases, so for higher order elements there is little need for special treatment of the blending elements.

The effects of the size of the crack tip enrichment domain has been studied by Ventura *et al* [108], Laborde *et al* [64] and Béchet *et al* [8]. They all observed that although in the original XFEM papers only the nodes nearest to a singularity were enriched, enriching a fixed geometric area around the singularity significantly improves the rate of convergence as the mesh is refined.

Convergence is studied in [64], where the role of the blending region between enriched and unenriched elements on the convergence rate is investigated. These results are revisited by Chahine *et al* [21] who introduces the concept of a cut-off or weight function for the enrichment. This concept has been lately fruitfully applied to solving blending issues, see section 9.

Several works have considered the determination of stress intensity factors. Since the early works, the stress intensity factors have been computed by the domain form of the J-integral [32, 52, 75, 79]. Liu *et al* [68] proposed a direct evaluation of the stress intensity factors, based on enrichment functions expressed in terms of stress intensity factors. A study of the performance of the contour integral, the cut-off function and the J-integral method can be found in [84]. Robust methods for evaluation of the J-integral have been described in Legrain *et al* [67]. In Duarte *et al* [35] a least squares fit of the GFEM stresses to the asymptotic crack tip fields was used to extract stress intensity factors.

3.3. Cohesive cracks

Cohesive cracks can be treated within the XFEM framework. Well and Sluys [113] used the step function enrichment to solve delamination problems in composites with a cohesive law. The crack tip progressed element by element.

To achieve good accuracy and the ability to deal with crack fronts within elements, special enrichments have been developed. In Moës and Belytschko [74], the following enrichments basis for two-dimensional crack tips was found to be effective

$$\{\Psi_i\}_{i=1}^3 = \{r\sin(\theta/2), r^{\frac{3}{2}}\sin(\theta/2), r^2\sin(\theta/2)\}. \tag{19}$$

Zi and Belystchko [119] presented a new crack tip element for cohesive cracks based on the sign function (generalized Heaviside step function). The crack tip can be located anywhere within an element. However the crack tip opening is linear, so it requires great resolution for elastic cracks and substantial resolution for cohesive cracks.

In [70] Mariani and Perego proposed to reproduce the cusp-like shape of the process zone by introducing a polynomial ramp multiplied by the generalized Heaviside step function. Applications of cohesive crack modeling in functionally graded materials have been presented by Comi and Mariani [27] and in concrete by Unger *et al* [104]. Cohesive models in the XFEM/GFEM framework have been discussed by de Borst *et al* [29, 30]. Other interesting developments for cohesive cracks can be found in [5, 11, 113].

4. Dislocations

Dislocations can be treated by XFEM by methods that are similar to those for cracks. These methods are based on the Volterra concept of a dislocation: the body is cut across a surface, the two sides of the surface are displaced relative to each other by the Burgers vector, and the surfaces are glued together. This problem can be posed as the analysis of a body containing an embedded surface of discontinuity where the relative displacements (or jump in displacements) across the surface of discontinuity are prescribed according to the Burgers vector $\boldsymbol{b}$ of the dislocation. XFEM has been applied to the mesoscale modeling of dislocations in two dimensions [12, 49, 50, 108], three dimensions [49, 82] and in thin shells such as carbon nanotubes [82].

To describe the XFEM approach to dislocations, we define the geometry of the dislocation by level sets, as we did for cracks. A dislocation loop is represented by two level sets, $f(\boldsymbol{x})$ and $g(\boldsymbol{x})$, as shown in figure 4. The glide plane is defined by the zero contour of $f(\boldsymbol{x})$ and the dislocation line is the intersection of $f(\boldsymbol{x}) = 0$ and $g(\boldsymbol{x}) = 0$. The sense of the dislocation line is then $\boldsymbol{\zeta} = \nabla f \times \nabla g$.

The approximations for a linear isotropic domain containing n^d Volterra dislocations is

$$\boldsymbol{u}^h(\boldsymbol{x}) = \boldsymbol{u}^{\text{FE}}(\boldsymbol{x}) + \sum_{\alpha=1}^{n^d} \boldsymbol{u}_\alpha^D(\boldsymbol{x}), \tag{20}$$
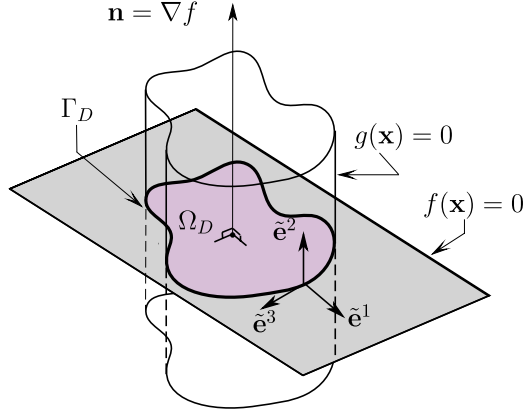
Figure 4. Level set description of a dislocation loop.

(This figure is in colour only in the electronic version)

where

$$\boldsymbol{u}_\alpha^D(\boldsymbol{x}) = \boldsymbol{b}_\alpha \sum_{I \in \mathcal{S}_\alpha^{\text{jump}}} N_I(\boldsymbol{x})(H(f_\alpha(\boldsymbol{x})g_\alpha(\boldsymbol{x})) - H_{\alpha I})$$

$$+ b^\alpha \sum_{I \in \mathcal{S}_\alpha^{\text{core}}} N_I(\boldsymbol{x})(\boldsymbol{u}_\alpha^{\text{core}}(f_\alpha(\boldsymbol{x}), g_\alpha(\boldsymbol{x})) - \boldsymbol{u}_{\alpha I}^{\text{core}}), \tag{21}$$

where $\boldsymbol{b}_\alpha$ is the Burgers vector of dislocation α, b_α is the magnitude of $\boldsymbol{b}_\alpha$, $\boldsymbol{u}_\alpha^{\text{core}}(f_\alpha(\boldsymbol{x}), g_\alpha(\boldsymbol{x}))$ is the asymptotic solution for a dislocation on a slip plane with normal ∇f_α and Burgers vector $b_\alpha^{-1}\boldsymbol{b}_\alpha$ and $\boldsymbol{u}_{\alpha I}^{\text{core}} = \boldsymbol{u}^{\text{core}}(f_\alpha(\boldsymbol{x}_I), g_\alpha(\boldsymbol{x}_I))$. The function $\boldsymbol{u}_\alpha^{\text{core}}(f_\alpha(\boldsymbol{x}), g_\alpha(\boldsymbol{x}))$ is given in [49, 82]. The set $\mathcal{S}_\alpha^{\text{core}}$ is the set of nodes within a certain radius of dislocation core α and $\mathcal{S}_\alpha^{\text{jump}}$ is the set of all nodes not in $\mathcal{S}_\alpha^{\text{core}}$ with supports cut by $f_\alpha(\boldsymbol{x}) = 0$ and $g_\alpha(\boldsymbol{x}) < 0$. The geometry of the discontinuity associated with the dislocation is completely independent of the FE mesh, so dislocations can be arbitrarily oriented with respect to the mesh.

The displacement approximation (21) closely resembles that for linear elastic cracks (3). By enriching nodes near the dislocation core with $\boldsymbol{u}^{\text{core}}(f(\boldsymbol{x}), g(\boldsymbol{x}))$, the XFEM solution can accurately capture the core singularity, which is analogous to the tip enrichment for cracks (6). Slip far from the dislocation core is captured by the Heaviside step function enrichment $H(z)$, which is the same enrichment used to model crack opening away from the crack tip.

The discrete equations for dislocations have the same form as those for linear elastic cracks, i.e. (8)–(16), but since the Burgers vector $\boldsymbol{b}$ is prescribed, the only free degrees of freedom are those of the standard finite element problem $\boldsymbol{u}_I$. Therefore the discrete equations for these dislocation methods are of the form

$$\boldsymbol{K}^{uu}\boldsymbol{d}^u = \boldsymbol{f}^{\text{ext}} - \sum_{i=0}^{1} \boldsymbol{K}^{ui}\boldsymbol{q}^i. \tag{22}$$

Furthermore, the stiffness matrix is independent of the number, orientation and location of the dislocations. This is advantageous in dislocation dynamics simulations because $\boldsymbol{K}^{uu}$ needs only to be computed and triangulated once at the beginning of a simulation, leading to significant savings in computations. In addition, since the effect of the dislocation appears only as a nodal force, the dislocation model is easily incorporated into commercial FE codes such as Abaqus and Ansys.
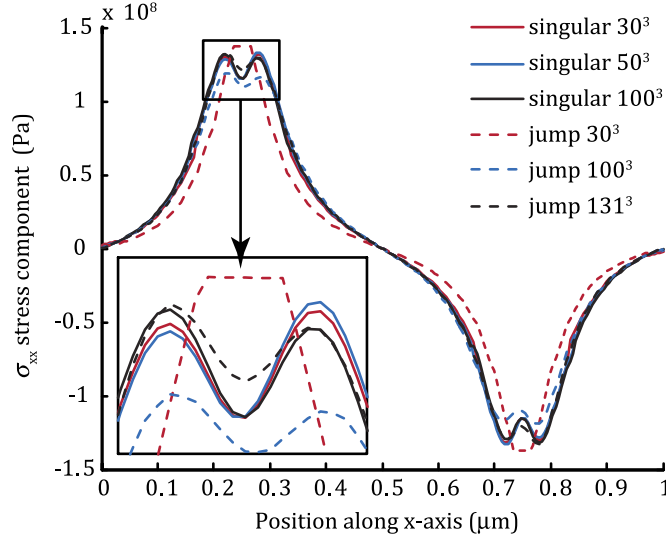
Figure 5. Comparison of the accuracy of the dislocation approximation with and without core enrichment for the problem of a circular dislocation loop of radius $r = 0.25\,\mu$m and Burgers vector $\boldsymbol{b} = (5\,\text{Å}, 0, 0)$ in a $1\,\mu$m $\times$ $1\,\mu$m $\times$ $1\,\mu$m cubic domain [82]. The mesh size is noted in the legend. (Reprinted with permission © Elsevier [82].)

Core enrichment functions are not readily available for problems involving nonlinear or anisotropic materials or for large displacement problems. Dislocations in such problems can be modeled by using only the step function enrichment. The displacement field approximation is then given by

$$\boldsymbol{u}(\boldsymbol{x}) = \boldsymbol{u}^{\text{FE}}(\boldsymbol{x}) + \boldsymbol{b} \sum_{I \in \mathcal{S}^{\text{jump}}} N_I(\boldsymbol{x})(\Psi(f(\boldsymbol{x}), g(\boldsymbol{x})) - \Psi_I), \tag{23}$$

where $\mathcal{S}^{\text{jump}}$ is the set of nodes of elements cut by the plane defined by $f(\boldsymbol{x}) = 0$ and $g(\boldsymbol{x}) < 0$, $\Psi_I = \Psi(f(\boldsymbol{x}_I), g(\boldsymbol{x}_I))$ and

$$\Psi(f(\boldsymbol{x}), g(\boldsymbol{x})) = G(g(\boldsymbol{x}))H(f(\boldsymbol{x})), \tag{24}$$

where $G(g)$ is a function which specifies the magnitude of the discontinuity across the slip plane. For a Volterra model, $G(g) = H(-g)$, but this displacement field is incompatible at the center of the core. This incompatibility can be eliminated by regularizing the step function as it approaches the core. It is also possible to circumvent this difficulty by a Peierls–Nabarro core model, which is accomplished by letting $G(g) = -\pi^{-1}\arctan(g/a)$, where a is a parameter related to the size of the core. $G(g)$ can also be chosen as a spline which has been fitted to an atomistic simulation.

The approximation (23) requires finer mesh resolution than a displacement field that includes core enrichment (20) for comparable accuracy. To illustrate this, figure 5 compares the x-direction stress for a dislocation loop in an infinite, linear, isotropic domain for models with and without core enrichment. It can be seen that with core enrichment a much coarser mesh of $30 \times 30 \times 30$ elements provides about the same accuracy as a $130 \times 130 \times 130$ element mesh that only employs the step enrichment. Of course, core enrichment is only feasible if near-field solutions are available, although they can often be constructed from finite element or atomistic solutions.

In dislocation dynamics simulations, the Peach–Koehler force which drives the motion of dislocations must be computed at each step of the simulation for each dislocation segment. For linear problems which use the approximation (20), the driving force on a dislocation segment β whose core is located at $\boldsymbol{x}_\beta$ can be computed by the Peach–Koehler formula

$$\boldsymbol{F}^{\mathrm{PK}}(\boldsymbol{x}_\beta) = \boldsymbol{\zeta}(\boldsymbol{x}_\beta) \times (\widetilde{\boldsymbol{\sigma}}(\boldsymbol{x}_\beta) \cdot \boldsymbol{b}_\beta), \tag{25}$$

where

$$\widetilde{\boldsymbol{\sigma}}(\boldsymbol{x}_\beta) = \boldsymbol{\sigma}(\boldsymbol{u}^{\mathrm{FE}}(\boldsymbol{x}_\beta)) + \sum_{\alpha \in \mathcal{A}_\beta} \boldsymbol{\sigma}(\boldsymbol{u}_\alpha^D(\boldsymbol{x}_\beta)) \tag{26}$$

and $\mathcal{A}_\beta$ is a small subset of all dislocations enrichment functions that are nonzero at $\boldsymbol{x}_\beta$, i.e. $\mathcal{A}_\beta = \{\alpha | \alpha \neq \beta, \exists I \in \mathcal{S}_\alpha^{\mathrm{core}}, \boldsymbol{x}_\beta \in \mathrm{supp}(N_I)\}$.

Equation (26) is similar to that used in superposition based dislocation models [80, 105], but it is more efficient since it only involves a sum over a small subset of the dislocations in the domain, i.e. those dislocations whose domains of enrichment include the location of the dislocation core for which the Peach–Koehler force is evaluated. In the XFEM dislocation model long-range interactions as well as the image stresses are captured by the standard FE part of the stress $\boldsymbol{\sigma}(\boldsymbol{u}^{\mathrm{FE}}(\boldsymbol{x}_\beta t))$. In classical superposition methods [80, 105], the Peach–Koehler force computation requires a sum over all dislocation segments in the model; the evaluation of this sum takes a significant fraction of the total computation time.

The Peach–Koehler force which determines dislocation motion can also be computed by the J-integral, and this approach appears to be necessary when the singular core enrichment is not included [12]. This is because the total stress field becomes singular at the core and the stress from other dislocations cannot be decoupled from the singular part of the total stress.

A major advantage of the XFEM approach to modeling dislocations, in comparison with methods based on analytic solutions or boundary integral methods, is its ability to deal with problems with complex geometry. Both the combined step and core enriched (20) and the step enriched (23) models are applicable to arbitrary geometries, i.e. they have the full flexibility of standard finite element methods. Moreover, the step function enrichment (23) is applicable to nonlinear and anisotropic problems. Some of the versatility of these methods is illustrated by the application of XFEM to dislocations in thin anisotropic films shown in figure 6. XFEM has also been applied to dislocations in carbon nanotubes. The dislocation enrichment functions for carbon nanotubes are constructed by mapping the two dimensional enrichment functions (20) onto a cylindrical manifold. The results obtained by this method compare well with fully atomistic simulations [82]. Some of the difficulties of accurately modeling core behavior in anisotropic materials can be overcome by coupling the XFEM dislocation model with an atomistic model at the dislocation cores, as in Gracie and Belytschko [48].

5. Grain boundaries

The complex geometries of grain boundaries can easily be modeled by XFEM/GFEM. The advantage of these methods lies in the fact that the mesh need not have any relationship to the geometry of the grain boundaries, whereas in a standard finite element method, element edges must be aligned with grain boundaries. This was illustrated in figure 2 in two dimensions.

The XFEM approximations for multibody problems with sliding interfaces were first constructed by Belytschko *et al* [15] for the analogous problem of jointed rock by using the Heaviside step function enrichment. Let the surface of grain i and its volume be defined by $f^{(i)}(\boldsymbol{x}) = 0$ and $f^{(i)}(\boldsymbol{x}) > 0$, respectively. Several types of enrichment have been used: with relative normal displacements allowed on the boundary or only relative slip allowed. When
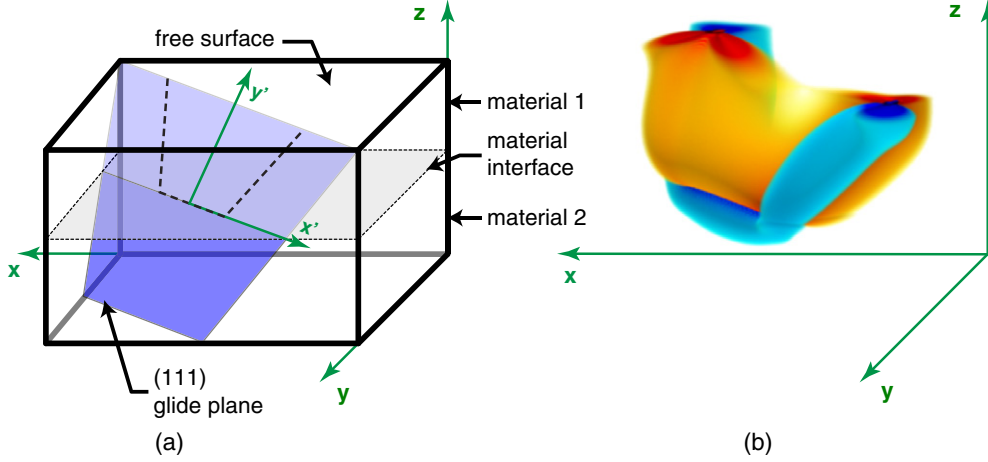
Figure 6. XFEM simulation of a threading dislocation in a SiGe thin film [82]. The dashed line denotes the dislocation line. (*a*) Dislocation and domain geometry. (*b*) The σ_{xx} stress resulting from the dislocation. (Reprinted with permission © Elsevier [82].)

only slip is allowed, the Heaviside step function is applied only to the tangential component, and the enrichment is

$$\boldsymbol{u}^{\mathrm{enr}} = \sum_{i\alpha} \boldsymbol{e}_\alpha^{(i)} \sum_I N_I(\boldsymbol{x})(H(f^{(i)}(\boldsymbol{x})) - H(f^{(i)}(\boldsymbol{x}_I)))q_{\alpha I} \tag{27}$$

where $\boldsymbol{e}_\alpha^{(i)}$ are the unit tangent vectors to the surface $f^{(i)}(\boldsymbol{x}) = 0$. For junctions of discontinuities, the techniques in Duarte [37] need to be used. The above displacement field is identical to that of the dislocation model (23), as can be seen by letting $\boldsymbol{b} = \sum_\alpha \boldsymbol{e}_\alpha^{(i)} q_{\alpha I}$ for all nodes I.

If normal separation between grains is to be modeled along the grain boundary by a cohesive law [118], then the displacement field for a grain boundary is identical to that for cracks (3), but without the crack tip enrichment. In addition, a penalty force or some other constraint technique must be applied to prevent interpenetration along the grain boundaries, see for example [33].

An alternative technique has been developed in the context of GFEM by Simone *et al* [90] which employs the enrichment

$$\boldsymbol{u}^{\mathrm{enr}}(\boldsymbol{x}) = \sum_I N_I(\boldsymbol{x}) \sum_\alpha^{n_G} \mathcal{H}_\alpha(\boldsymbol{x})\boldsymbol{u}_{\alpha I}, \tag{28}$$

where n_G is the number of grains and

$$\mathcal{H}_\alpha(\boldsymbol{x}) = \begin{cases} 1, & \text{if } \boldsymbol{x} \text{ is in grain } \alpha, \\ 0, & \text{otherwise} \end{cases}. \tag{29}$$

The basis of this field is identical to the XFEM basis for discontinuities. The advantage of this form of the enrichment is that junctions involving three or more boundaries can be handled more conveniently, since the form (27) requires additional basis functions at junctions, see [15, 28]. The enrichment (28) includes one linear dependent function for every node with a support cut by a grain; however, this linear dependence can be removed using a modification of (28), as described in [90]. Simone *et al* [90] formulated the approximation for discontinuities in

13

the total field but only applied the approximation to problems where the tangential component is unconstrained.

6. Phase interfaces

XFEM and GFEM have been used to solve problems of evolving interfaces; in these applications they are often combined with level set methods for tracking interfaces. On interfaces, in contrast to the problems described so far, the gradient of the primary variable (often the displacement) is discontinuous but the variable itself is continuous. A typical application is the modeling of inclusions. In standard finite element methods, it is necessary that element edges coincide with the phase interfaces because otherwise the accuracy of the finite element solution is significantly compromised. Many problems have been solved with finite element models where the properties of elements on the interface are determined according to a Voigt law of homogenization [121]. However, convergence studies show that these methods do not converge at the optimal rate.

The simplest enrichment function used by the XFEM to introduce a discontinuity into the gradient of the approximation is the absolute value function (also called the *ridge* or *tent* function). Let $f(x)$ be a signed distance function to the interface; in this case the enrichment is

$$u^{\mathrm{enr}}(x) = \sum_I N_I(x)|f(x)|q_I, \tag{30}$$

i.e. the absolute value of the level set function is used as the enrichment. This idea of introducing a ridge to model discontinuous gradients was first proposed in the context of meshfree methods by Krongauz and Belytschko [62]. Extensions to finite elements in terms of level set functions were developed in [15, 98]. Note that for this enrichment, the use of level sets is almost indispensable, since it is difficult to define a ridge function without them.

The ridge enrichment is more troublesome than the Heaviside enrichment because even with shifting, it does not vanish at the edges of the elements crossed by the discontinuity. Furthermore, parasitic behavior is introduced by the approximation in the blending elements unless special techniques are used. These issues are discussed in detail in section 9.

Modeling of the evolution of phase boundaries is most conveniently handled by combining XFEM with level set methods. Such applications were first proposed in Chessa and Belytschko [22–24]. The use of level sets is already implicit in (30); some more details are given in the next section.

Approximations for gradient discontinuities within elements can also be constructed by constraining discontinuous approximations. For example, if we start with the approximation for a crack (3) without tip enrichment and then constrain the displacement field to be continuous along the line $f(x) = 0$ (i.e the discontinuity), the resulting field will be continuous but its gradient will be discontinuous along $f(x) = 0$. The continuity constraint can be imposed either by Lagrange multipliers or by Nitsche's method [60, 78]. This type of approximation was first proposed by Hansbo and Hansbo [53].

Merle and Dolbow [73] have considered thermal and phase change problems in one dimension by these methods. They use the Heaviside step function enrichment and then apply the continuity constraint. They report that the accuracy of this approach is significantly better than the ridge function approach. Ji *et al* [59] have proposed XFEM methods for phase transitions using the fast marching method; Hermitian polynomials were used for the dependent variable of the primary problem. Zabaras *et al* [117] have used XFEM in conjunction with level sets and the ridge function to solve several interesting problems in dendritic solidification.

7. Level sets

The Level Set Method, Sethian *et al* [88] and Osher and Fedkiw [81], has become a key ingredient of XFEM. It allows for the complicated geometry of a feature such as a crack to be described by a simple functional representation. In addition, level sets allow the enrichment functions to be evaluated in a straightforward manner.

For example with a level set description of a crack, the crack surface can be defined by scalar values at the finite element nodes and by the FE shape functions, i.e. a level set $f(\boldsymbol{x}, t)$ can be defined as

$$f(\boldsymbol{x}, t) = \sum_I N_I(\boldsymbol{x}) f_I(t). \tag{31}$$

The evolution of the surfaces can then be accomplished by solving a hyperbolic evolution equation that governs the level sets, which is

$$\frac{\partial f(\boldsymbol{x})}{\partial t} + \boldsymbol{v}(\boldsymbol{x}) \cdot \boldsymbol{\nabla} f(\boldsymbol{x}) = 0, \tag{32}$$

where $\boldsymbol{v}$ is the velocity of the level set field. This velocity field must often be determined by projecting the velocity of the surface $f(\boldsymbol{x}) = 0$ throughout the domain. The fast marching method has been found to be an extremely efficient method for velocity projection in three-dimensional fracture simulations [97] and in applications of evolving biofilm interfaces [38].

The level set approach can dramatically simplify the solution of many problems, such as interface evolution, dislocation evolution and crack growth. However, it should be mentioned that in the application of level sets to cracks, the update of level sets still poses difficulties. One difficulty arises because the crack surface must be frozen once it develops. This cannot be easily handled under the conventional level set framework, though some progress is being made. Another difficulty is that the finite element meshes used for solution of the field equations are often inadequate for accurately solving the hyperbolic equation (32), so another mesh, often a finite difference mesh, is used for the level set update.

Applications of level sets and XFEM to crack growth in two dimensions were first described by Stolarska *et al* [94] and Belytschko *et al* [15] and for three-dimensional cracks in [76, 52]. The issue of freezing the level set for cracks was addressed in [52], although not completely satisfactorily. The hyperbolic equations for the level set update were solved by the characteristic Galerkin method. In Sukumar *et al* [99] a fast marching method was developed for updating the level sets of cracks in three dimensions. A geometric/vector point of view of the level set description and evolution of cracks was introduced in Ventura *et al* [106]. This method addresses the irreversibility of crack surfaces by using geometric updates; it also eliminates the need for solving differential equation (32) for the evolution of the level set. These ideas have been further developed by Sukumar *et al* [97] where a faster and more reliable level set update is described. Applications of XFEM and level sets to problems with multiple intersecting and branching cracks can be found in Budyn *et al* [20], Zi *et al* [120] and Loehnert and Belytschko [69]. Other relevant papers are [39] and [58].

8. Quadrature in XFEM/GFEM

An important issue in the implementation of XFEM and GFEM is the quadrature of the weak form. In standard finite elements, the evaluation of the element stiffness and the other terms of the weak form usually requires the quadrature of functions that are polynomials, which is easily accomplished with low order Gauss quadrature. When the approximation space is enriched by singular or discontinuous functions, these quadrature techniques need to be

modified because inaccurate quadrature can lead to inaccuracy and poor convergence of the XFEM/GFEM solutions [10, 75, 95, 96].

Several different approaches have been used in the literature to perform this task. Some of the methods are

- higher order Gauss quadrature, which has been demonstrated to perform quite poorly [95];
- adaptive quadrature for singular functions [95];
- subdomain quadrature, in which the element is subdivided into quadrature subdomains with boundaries aligned with the discontinuity (e.g. the crack faces or an interface between materials) where a fixed order Gauss rule is used [10, 75]. For singular enrichments this method requires special quadrature rules.
- transformation to a line integral or surface integral in two and three dimensions, respectively [107].

Special methods for cracks, based on a polar mapping of the integrand functions and domain, have been proposed by Laborde *et al* [64] and Béchet *et al* [8] and have been named *almost polar integration* and *singular mapping*, respectively. The first maps an ordinary quadrature rule on a square into a triangular domain, while the second exploits the structure of the enrichment functions to define a quadrature rule on a triangle. These two quadrature rules perform much better than standard Gauss quadrature, but they require a subdivision of the element containing the crack tip into triangles with vertices coincident with the crack tip.

A method for the step function enrichment that avoids subdividing the elements cut by the discontinuity was introduced by Ventura [109]. Here the enrichment functions are mapped to equivalent polynomials that can be easily integrated by a standard Gauss rule on the entire element domain. These polynomials are defined so as to give the exact result, using coefficients that are functions of the location of the discontinuity in the element. A related approach has been proposed by Holdych *et al* [55]. Here, starting with a given integration rule, quadrature weights are found, depending on the position of the discontinuity inside the element. The methods proposed in [55, 109] give the exact element stiffness, so it follows that the weights determined in [55] are related to the values of the equivalent polynomials [109] at the quadrature points.

Ventura *et al* [107] reduced the computational cost of the quadrature of singular enrichment functions for enrichment functions that satisfy the equilibrium equations. The divergence theorem was used to transform the element domain integral of the weak form into a boundary integral over the element edges. This approach was used for crack and dislocation problems, and proved quite effective.

9. Blending of enriched and non-enriched elements

Local partition of unity enrichments as introduced in Belytschko and Black [10] and Moës *et al* [75] have the advantage that they substantially reduce the number of variables in the global problem compared with full domain enrichments and improve the conditioning of the numerical problem. It should be stressed that there are no difficulties in the blending of the shifted Heaviside enrichment, because that enrichment vanishes along the edges of the elements cut by the discontinuity. On the other hand for other enrichments, such as ridge enrichments or tip enrichments, the transition from enriched to unenriched elements requires some care.

Consider a four-node quadrilateral blending element (like the cross-hatched elements in figure 3) adjacent to a tip enriched element. While all of the nodes of the enriched element are

enriched, only two of the nodes of the blending element are enriched. As a consequence in the blending element, the shape functions $N_K(\boldsymbol{x})$, $K \in \mathcal{S}_C$, no longer form a partition of unity. This can lead to errors in the blending elements and decreases in the rate of convergence.

In Sukumar *et al* [98], errors in the blending elements were found to degrade the convergence rate of solutions with the ridge enrichment function (30). A modification of the ridge enrichment function was proposed that improved the convergence rate. The issue of blending was further investigated by Chessa *et al* [25] who observed that the errors are caused by parasitic terms in the approximation space of the blending elements. They developed an assumed strain method whereby the parasitic strains in the blending elements are eliminated. The drawback of this approach is that special assumed strain elements need to be developed that depend on the enrichment and element types.

Another approach for circumventing the blending problem is to join the enriched and unenriched subdomains by interface conditions. Following this viewpoint, Gracie *et al* [51] introduced a patch-based version of the discontinuous Galerkin formulation, which enforces continuity between the enriched and unenriched patches by an interior penalty method. The resulting formulation, called DG-XFEM, is more accurate than the standard XFEM and achieves optimal convergence rates. Unlike assumed strain blending, this method does not require the development of new elements for the blending region.

Recently an effective and simple approach has been proposed by Fries [46] who used a linearly decreasing weight function for the enrichment in the blending elements. This approach allows one to obtain a conforming approximation and to eliminate partially enriched elements, so that the partition of unity property is satisfied everywhere. The idea of weighting the enrichment was also presented in [21] but with no reference to blending and also in [45] for governing the transition between finite elements and a moving least squares approximation. This approach has been extended in [107], where a more general ramp function was used and the influence of the weight function derivatives has been studied, as well as different enrichments. Blending the enrichment functions with a ramp function has proved very effective, simple to implement and appears to be a very satisfactory solution to blending difficulties.

10. Localization, damage and transition to fracture

The partition of unity concept has also been used for nonlocal and gradient models. Patzak and Jirasek [83] applied the XFEM step enrichment to model narrow damage localization zones. Damage was modeled by enriching the displacement field with a set of regularized Heaviside step functions, representing different internal length scales arranged in geometrical progression. The displacement is therefore continuous in the damaged zone, but the strains can be large and with a very steep gradient.

Simone *et al* [91] developed an implicit gradient-enhanced continuum damage model enriched with discontinuous interpolations activated at high damage to simulate material fracture. This approach was motivated by the observation that nonlocal continuum damage models, in either integral or differential form, deteriorate close to failure as these models are unable to represent discrete failure surfaces. As pointed out by the authors, the shortcomings of their approach are the incorrect energy dissipation at the onset of fracture and discontinuities in the response due to the sharp variation of the nonlocal interaction domains.

An energy conservation criterion has been proposed for mode I cracks by Comi *et al* [26], where the transition from damage to fracture is defined through an energy balance in such a way that the residual energy in the damage band is transferred to the cohesive crack interface. They present an estimate of the minimum number of elements required to resolve the localization band for a given accuracy by perturbation analysis.

In the framework of the regularized step function approach introduced by Patzak and Jirasek [83], Benvenuti *et al* [17] proposed a different mechanical model where the bulk strain field and the localized strain field are assumed to govern distinct mechanically uncoupled mechanisms. A bounded spring-like model is assumed for the localized constitutive law, so that its mechanical work converges to the traction–separation work when the regularization parameter vanishes, i.e. at fracture. The integration of the very steep gradients arising when the regularization parameter vanishes, i.e. close to fracture, is approached by the equivalent polynomial technique, so that the element stiffness is correctly evaluated with low order Gauss quadrature [109].

11. Other forms of discontinuous approximations

Hansbo and Hansbo [53] proposed a different form for representing displacement discontinuities. In their method, when a crack crosses an element e another element $\bar{e}$ is superimposed on e. In elements cut by the crack, the standard FE displacement field is replaced by

$$u^h(x) = \sum_{I \in e} u_I^e N_I^e(x) H(f(x)) + \sum_{I \in \bar{e}} u_I^{\bar{e}} N_I^{\bar{e}}(x)(1 - H(f(x))). \tag{33}$$

This corresponds to adding an extra element (and extra nodes) for every element that is crossed by a discontinuity. Integration of the weak form over these elements still requires special algorithms, as described in section 8, since the step function appears in the displacement field.

Areias and Belytschko [3] showed that Hansbo and Hansbo's approximation basis is a linear combination of the XFEM basis for discontinuities. So the performance is identical; the choice depends primarily on implementational aspects, and there do not seem to be particularly strong arguments in favor of either approach, though the XFEM form is more compatible with singularity enrichments.

Previously, Iarve [57] introduced an element based on polynomial B-splines for the step function discontinuity. Iarve's displacement field is of the form

$$u^h(x) = \bar{H}(f(x))u^{(1)}(x) + (1 - \bar{H}(f(x)))u^{(2)}(x) + u^{(3)}(x), \tag{34}$$

where $\bar{H}$ is a regularized step function,

$$u^{(1)}(x) = \sum_{I \in \Omega_e} N_I(x)u_I^{(1)}, \tag{35}$$

$$u^{(2)}(x) = \sum_{I \in \Omega_e} N_I(x)u_I^{(2)}, \tag{36}$$

$$u^{(3)}(x) = \sum_{I \in \Omega/\Omega_e} N_I(x)u_I^{(3)} \tag{37}$$

and Ω_e is the set of nodes of elements cut by the discontinuity.

An advantage of this method is that the step function is regularized by a spline, so that traditional Gaussian quadrature can be used. Issues related to quadrature in PUMs were described in section 8. Note that Iarve's form [57] is identical to that of Hansbo and Hansbo [53], if the step function is not regularized.

Fries and Belytschko [45] proposed a discontinuity enrichment that does not require additional degrees of freedom at nodes whose elements are crossed by the discontinuity. An approximation space consisting of discontinuity enriched moving least squares [14] is

constructed near discontinuities. The method is more complex than the standard XFEM enrichment for discontinuities, but its avoidance of extra degrees of freedom is sometimes an advantage.

The XFEM approach to fracture analysis is closely related to the s-method of Fish [40, 42, 43]. In the s-method, a mesh of elements is superimposed on the regular mesh. The superimposed elements are meshed so that they conform to the shape of the crack and double nodes are included on the crack surface to represent the discontinuity. Quarter point singular elements are used at the crack tip. These methods have the same quadrature difficulties as XFEM.

Lee *et al* [65] combined XFEM with the s-method of Fish [43] for modeling of stationary and growing cracks. Quarter points elements were superimposed on a background mesh but in contrast to Fish [43], the rest of the discontinuity was described by the step function enrichment.

11.1. Dynamic fracture and other topics

The simulation of dynamic fracture by PUM for softening materials which transition to a discontinuity was proposed by Wells *et al* [112, 111]. A similar method based on XFEM was developed in Belytschko *et al* [11] where a cohesive zone model used to model the crack tip behavior and a loss of hyperbolicity criterion was used to advance the crack. A special element was developed for partially cracked elements, but no tip enrichment was used. Réthoré *et al* [86, 87] have developed energy conserving time integration schemes for propagating cracks modeled by XFEM.

An alternative method for dynamic crack propagation based on the Hansbo and Hansbo [53] approach was developed in Song *et al* [92]. It was called the phantom node method, since an overlaid element and 'phantom nodes' were added to elements that cracked. They have developed efficient one-point quadrature rules for four-node quadrilaterals that avoid subdomain integration with little loss in accuracy. Shear bands were also treated by the XFEM in that paper.

Partition of unity enrichments have also been used in conjunction with multiscale approaches and homogenization theories, for both traditional small displacement/strain elasticity [41] and for nonlinear problems [42]. Two overlaid models were used, one defined on the large scale and one defined for small scale features like cracks, coupled by boundary conditions. It can be seen as an application of the partition of unity concept to the s-version of the finite element method [43]. A similar approach has been recently proposed for GFEM by Duarte and Kim [36].

XFEM has recently been applied to concurrent continuum-atomistic simulations of cracks and dislocations by Gracie and Belytschko [48]. The introduction of XFEM into the multiscale framework results in a substantial reduction in the number of atomistic degrees of freedom compared with a standard bridging domain method framework [16, 116].

XFEM has been applied to bimaterial problems by Sukumar *et al* [100], Hettich *et al* [54] and Huynh and Belytschko [56]. In the latter, both the crack and the interface were described by level sets. Béchet *et al* [9] have applied enrichments for cracks in piezoelectric materials. Enrichment functions with variable parameters were introduced in [110]. Here the enrichment function is adapted locally to the physics of a problem by determining the parameters giving the best solution. The parameters are determined iteratively starting from trial parameters, and the solutions are determined iteratively using an *a posteriori* error estimate.

Bordas *et al* [19] have developed object-oriented libraries for XFEM. The implementation of XFEM within a general purpose FEM code has been discussed by Sukumar and Prévost [102].

19

An important improvement that is needed in XFEM is adaptivity. For this purpose, error estimators will need to be developed. Bordas and Duflot [18] have developed error estimators based on L_2 projections.

12. Conclusions

The major concepts of XFEM/GFEM have been reviewed along with their history and their major applications. The most mature field of applications is the modeling of stationary and evolving cracks. These applications have reached a high degree of robustness and are now being incorporated into general purpose codes such as LS-DYNA and ABAQUS. Applications to grain boundaries and dislocations are still embryonic, although these applications share a similar conceptual and implementational framework. The payoffs in applying these technologies to grain boundaries would be quite substantial because they would facilitate the study of real grain boundary configurations in three dimensions, the effects of anisotropy, nonlinearities, etc.

The combination of XFEM/GFEM with level sets has also enhanced their capabilities, since this makes possible the description of cracks, dislocations, grain boundaries and phase interfaces strictly in terms of nodal data. Furthermore, it enables one to harness the powerful level set methods that have been developed to track the evolution of these surfaces.

The XFEM/GFEM framework also provides a powerful tool for enriching solution spaces with information from asymptotic solutions and other knowledge of the physics of the problem. This has proved very useful for elastic cracks and dislocations, where near-field solutions can be embedded by the PUM to tremendously increase the accuracy of relatively coarse meshes. It also offers possibilities in treating phenomena such as surface effects in nanomechanics, void growth, subscale models of interface behavior, etc.

Thus in total, the XFEM/GFEM have tremendously enhanced the power of finite element methods for many of the problems of interest in the mechanics of materials. The development of XFEM/GFEM is still in its early stages, and many promising applications remain to be made.

Acknowledgments

References

[1] Abdelaziz Y and Hamouine A 2008 A survey of the extended finite element *Comput. Struct.* **86** 1141–51

[2] Areias P M A and Belytschko T 2005 Analysis of three-dimensional crack initiation and propagation using the extended finite element method *Int. J. Numer. Methods Eng.* **63** 760–88

[3] Areias P M A and Belytschko T 2006 A comment on the article 'a finite element method for simulation of strong and weak discontinuities in solid mechanics' by A Hansbo and P Hansbo (2004 *Comput. Methods Appl. Mech. Eng.* **193** 3523—40) *Comput. Methods Appl. Mech. Eng.* **195** 1275–6

[4] Asadpoure A and Mohammadi S 2007 Developing new enrichment functions for crack simulation in orthotropic media by the extended finite element method *Int. J. Numer. Methods Eng.* **68** 2150–72

[5] Asferg J L, Poulsen P N and Nielsen L O 2007 A consistent partly cracked XFEM element for cohesive crack growth *Int. J. Numer. Methods Eng.* **72** 464–85

[6] Babuška I, Banerjee U and Osborn J E 2003 Survey of meshless and generalized finite element methods: a unified approach *Acta Numer.* **12** 1–125

[7] Babuška I, Caloz G and Osborn J E 1994 Special finite element methods for a class of second order elliptic problems with rough coefficients *SIAM J. Numer.l Anal.* **31** 945

[8] Béchet E, Minnebo H, Moës N and Burgardt B 2005 Improved implementation and robustness study of the X-FEM for stress analysis around cracks *Int. J. Numer. Methods Eng.* **64** 1033–56

[9] Béchet E, Scherzer M and Kuna M 2009 Application of the X-FEM to the fracture of piezoelectric materials *Int. J. Numer. Methods Eng.* **77** 1535–65

[10] Belytschko T and Black T 1999 Elastic crack growth in finite elements with minimal remeshing *Int. J. Numer. Methods Eng.* **45** 601–20

[11] Belytschko T, Chen H, Xu J and Zi G 2003 Dynamic crack propagation based on loss of hyperbolicity and a new discontinuous enrichment *Int. J. Numer. Methods Eng.* **58** 1873–905

[12] Belytschko T and Gracie R 2007 On XFEM applications to dislocations in problems with interfaces *Int. J. Plast.* **23** 1721–38

[13] Belytschko T, Krongauz Y, Organ D, Fleming M and Krysl P 1996 Meshless methods: an overview and recent developments *Comput. Methods Appl. Mech. Eng.* **139** 3–47

[14] Belytschko T, Lu Y Y and Gu L 1994 Element-free Galerkin methods *Int. J. Numer. Methods Eng.* **37** 229–56

[15] Belytschko T, Moës N, Usui S and Parimi C 2001 Arbitrary discontinuities in finite elements *Int. J. Numer. Methods Eng.* **50** 993–1013

[16] Belytschko T and Xiao S P 2003 Coupling methods for continuum model with molecular model *Int. J. Multiscale Comput. Eng.* **1** 115–26

[17] Benvenuti E, Tralli A and Ventura G 2008 A regularized XFEM model for the transition from continuous to discontinuous displacements *Int. J. Numer. Methods Eng.* **74** 911

[18] Bordas S and Duflot M 2007 Derivative recovery and *a posteriori* error estimate for extended finite elements *Comput. Methods Appl. Mech. Eng.* **196** 3381–99

[19] Bordas S, Nguyen P V, Dunant C, Guidoum A and Nguyen-Dang H 2007 An extended finite element library *Int. J. Numer. Methods Eng.* **71** 703

[20] Budyn E, Zi G, Moës N and Belytschko T 2004 A method for multiple crack growth in brittle materials without remeshing *Int. J. Numer. Methods Eng.* **61** 1741–70

[21] Chahine E, Laborde P and Renard Y 2006 A quasi-optimal convergence result for fracture mechanics with XFEM *C. R.—Math.* **342** 527–32

[22] Chessa J and Belytschko T 2003 An enriched finite element method and level sets for axisymmetric two-phase flow with surface tension *Int. J. Numer. Methods Eng.* **58** 2041–64

[23] Chessa J and Belytschko T 2003 An extended finite element method for two-phase fluids *J. Appl. Mech.—Trans. ASME* **70** 10–17

[24] Chessa J, Smolinski P and Belytschko T 2002 The extended finite element method (XFEM) for solidification problems *Int. J. Numer. Methods Eng.* **53** 1959–77

[25] Chessa J, Wang H and Belytschko T 2003 On the construction of blending elements for local partition of unity enriched finite elements *Int. J. Numer. Methods Eng.* **57** 1015–38

[26] Comi C, Mariani S and Perego U 2007 An extended FE strategy for transition from continuum damage to mode I cohesive crack propagation *Int. J. Numer. Methods Geomech.* **31** 213

[27] Comi C and Mariani S 2007 Extended finite element simulation of quasi-brittle fracture in functionally graded materials *Comput. Methods Appl. Mech. Eng.* **196** 4013–26

[28] Daux C, Moes N, Dolbow J, Sukumar N and Belytschko T 2000 Arbitrary branched and intersecting cracks with the extended finite element method *Int. J. Numer. Methods Eng.* **48** 1741–60

[29] de Borst R, Gutiérrez M A, Wells G N, Remmers J J C and Askes H 2004 Cohesive-zone models, higher-order continuum theories and reliability methods for computational failure analysis *Int. J. Numer. Methods Eng.* **60** 289–315

[30] de Borst R, Remmers J J C and Needleman A 2006 Mesh-independent discrete numerical representations of cohesive-zone models *Eng. Fract. Mech.* **73** 160–77

[31] Dolbow J, Moës N and Belytschko T 2000 Discontinuous enrichment in finite elements with a partition of unity method *Finite Elements Anal. Des.* **36** 235–60

[32] Dolbow J, Moës N and Belytschko T 2000 Modeling fracture in Mindlin–Reissner plates with the extended finite element method *Int. J. Solids Struct.* **37** 7161–83

[33] Dolbow J, Moës N and Belytschko T 2001 An extended finite element method for modeling crack growth with frictional contact *Comput. Methods Appl. Mech. Eng.* **190** 6825–46

[34] Duarte C A, Babuška I and Oden J T 2000 Generalized finite element methods for three-dimensional structural mechanics problems *Comput. Struct.* **77** 215–32

[35] Duarte C A, Hamzeh O N, Liszka T J and Tworzydlo W W 2001 A generalized finite element method for the simulation of three-dimensional dynamic crack propagation *Comput. Methods Appl. Mech. Eng.* **190** 2227–62

[36] CA Duarte and Kim D J 2008 Analysis and applications of a generalized finite element method with global–local enrichment functions *Comput. Methods Appl. Mech. Eng.* **197** 487–504

[37] Duarte C A and Oden J T 1996 An hp adaptive method using clouds *Comput. Methods Appl. Mech. Eng.* **139** 237–62

[38] Duddu R, Bordas S, Chopp D and Moran B 2008 A combined extended finite element and level set method for biofilm growth *Int. J. Numer. Methods Eng.* **74** 848–70

[39] Duflot M 2007 A study of the representation of cracks with level sets *Int. J. Numer. Methods Eng.* **70** 1261–302

[40] Fan R and Fish J 2008 The rs-method for material failure simulations *Int. J. Numer. Methods Eng.* **73** 1607

[41] Fish J and Yuan Z 2005 Multiscale Enrichment based on Partition of Unity *Int. J. Numer. Methods Eng.* **62** 1341–59

[42] Fish J and Yuan Z 2007 Multiscale enrichment based on partition of unity for nonperiodic fields and nonlinear problems *Comput. Mech.* **40** 249–59

[43] Fish J 1992 The s-version of the finite element method *Comput. Struct.* **43** 539–47

[44] Fleming M, Chu Y A, Moran B and Belytschko T 1997 Enriched element-free Galerkin methods for crack tip fields *Int. J. Numer. Methods Eng.* **40** 1483–504

[45] Fries T P and Belytschko T 2006 The intrinsic XFEM: a method for arbitrary discontinuities without additional unknowns *Int. J. Numer. Methods Eng.* **68** 1358–85

[46] Fries T P 2008 A corrected xfem approximation without problems in blending elements *Int. J. Numer. Methods Eng.* **75** 503–32

[47] Gasser T C and Holzapfel G A 2005 Modeling 3D crack propagation in unreinforced concrete using PUFEM *Comput. Methods Appl. Mech. Eng.* **194** 2859–96

[48] Gracie R and Belytschko T 2009 Concurrently coupled atomistic and xfem models for dislocations and cracks *Int. J. Numer. Methods Eng.* doi:10.1002/nme.2488

[49] Gracie R, Oswald J and Belytschko T 2008 On a new extended finite element method for dislocations: core enrichments *J. Mech. Phys. Solids* **56** 200–14

[50] Gracie R, Ventura G and Belytschko T 2007 A new fast method for dislocations based on interior discontinuities *Int. J. Numer. Methods Eng.* **69** 423–41

[51] Gracie R, Wang H and Belytschko T 2008 Blending in the extended finite element method by discontinuous galerkin and assumed strain methods *Int. J. Numer. Methods Eng.* **74** 1645–69

[52] Gravouil A, Moes N and Belytschko T 2002 Non-planar 3D crack growth by the extended finite element and level sets: II. Level set update *Int. J. Numer. Methods Eng.* **53** 2569–86

[53] Hansbo A and Hansbo P 2004 A finite element method for the simulation of strong and weak discontinuities in solid mechanics *Comput. Methods Appl. Mech. Eng.* **193** 3523–40

[54] Hettich T, Hund A and Ramm E 2008 Modeling of failure in composites by x-fem and level sets within a multiscale framework *Comput. Methods Appl. Mech. Eng.* **197** 414–24

[55] Holdych D J, Noble D R and Secor R B 2008 Quadrature rules for triangular and tetrahedral elements with generalized functions *Int. J. Numer. Methods Eng.* **73** 1310–27

[56] Huynh D B P and Belytschko T 2009 The extended finite element method for fracture in composite materials *Int. J. Numer. Methods Eng.* **77** 214–39

[57] Iarve E V 2003 Mesh independent modeling of cracks by using higher order shape functions *Int. J. Numer. Methods Eng.* **56** 869–82

[58] Jäger P, Steinmann P and Kuhl E 2008 On local tracking algorithms for the simulation of three-dimensional discontinuities *Comput. Mech.* **42** 395–406

[59] Ji H, Chopp D and Dolbow J E 2002 A hybrid extended finite element/level set method for modeling phase transformations *Int. J. Numer. Methods Eng.* **54** 1209–33

[60] Ji H and Dolbow J E 2004 On strategies for enforcing interfacial constraints and evaluating jump conditions with the extended finite element method *Int. J. Numer. Methods Eng.* **61** 2508–35

[61] Karihaloo B L and Xiao Q Z 2003 Modelling of stationary and growing cracks in FE framework without remeshing: a state-of-the-art review *Comput. Struct.* **81** 119–29

[62] Krongauz Y and Belytschko T 1998 Efg approximation with discontinuous derivatives *Int. J. Numer. Methods Eng.* **41** 1215–33

[63] Krysl P and Belytschko T 1999 The element free Galerkin method for dynamic propagation of arbitrary 3-D cracks *Int. J. Numer. Methods Eng.* **44** 767–80

[64] Laborde P, Pommier J, Renard Y and Salaun M 2005 High order extended finite element method for cracked domains *Int. J. Numer. Methods Eng.* **64** 354–81

[65] Lee S H, Song J H, Yoon Y C, Zi G and Belytschko T 2004 Combined extended and superimposed finite element method for cracks *Int. J. Numer. Methods Eng.* **59** 1119–36

[66] Legay A, Wang H W and Belytschko T 2005 Strong and weak arbitrary discontinuities in spectral finite elements *Int. J. Numer. Methods Eng.* **64** 991–1008

[67] Legrain G, Moës N and Verron E 2008 Robust and direct evaluation of J_2 in linear elastic fracture mechanics with the X-FEM *Int. J. Numer. Methods Eng.* **76** 1471–88

[68] Liu X Y, Xiao Q Z and Karihaloo B L 2004 XFEM for direct evaluation of mixed mode SIFs in homogeneous and bi-materials *Int. J. Numer. Methods Eng.* **59** 1103–18

[69] Loehnert S and Belytschko T 2007 A multiscale projection method for macro/microcrack simulations *Int. J. Numer. Methods Eng.* **71** 1466–82

[70] Mariani S and Perego U 2003 Extended finite element method for quasi-brittle fracture *Int. J. Numer. Methods Eng.* **58** 103–26

[71] Melenk J M and Babuška I 1996 The partition of unity finite element method: basic theory and applications *Comput. Methods Appl. Mech. Eng.* **39** 289–314

[72] Melenk J M 1995 On generalized finite element methods *PhD Thesis* University of Maryland

[73] Merle R and Dolbow J 2002 Solving thermal and phase change problems with the extended finite element method *Comput. Mech.* **28** 339–50

[74] Moës N and Belytschko T 2002 Extended finite element method for cohesive crack growth *Eng. Fract. Mech.* **69** 813–33

[75] Moës N, Dolbow J and Belytschko T 1999 A finite element method for crack growth without remeshing *Int. J. Numer. Methods Eng.* **46** 131–50

[76] Moës N, Gravouil A and Belytschko T 2002 Non-planar 3D crack growth by the extended finite element and level sets: I. Mechanical model *Int. J. Numer. Methods Eng.* **53** 2549–68

[77] Mohammadi S 2008 *Extended Finite Element Method for Fracture Analysis of Structures* (Oxford: Blackwell)

[78] Mourad H M, Dolbow J and Harari I 2007 A bubble-stabilized finite element method for dirichlet constraints on embedded interfaces *Int. J. Numer. Methods Eng.* **69** 772–93

[79] Nagashima T, Omoto Y and Tani S 2003 Stress intensity factor analysis of interface cracks using X-FEM *Int. J. Numer. Methods Eng.* **56** 1151–73

[80] O'Day M P and Curtin W A 2005 A superposition framework for discrete dislocation plasticity *J. Appl. Mech.* **71** 805

[81] Osher S and Fedkiw R P 2003 *Level Set Methods and Dynamic Implicit Surfaces* (Berlin: Springer)

[82] Oswald J, Gracie R, Khare R and Belytschko T 2009 An extended finite element method for dislocations in complex geometries: thin films and nanotubes *Comput. Methods Appl. Mech. Eng.* at press, doi:10.1016/j.cma.2008.12.025

[83] Patzák B and Jirásek M 2003 Process zone resolution by extended finite elements *Eng. Fract. Mech.* **70** 957–77

[84] Pereira J P and Duarte C A 2005 Extraction of stress intensity factors from generalized finite element solutions *Eng. Anal. Bound. Elem.* **29** 397–413

[85] Rabczuk T, Bordas S and Zi G 2009 On three-dimensional modelling of crack growth using partition of unity methods *Comput. Struct.* at press, doi:10.1016/j.compstruc.2008.08.010

[86] Réthoré J, Gravouil A and Combescure A 2005 An energy-conserving scheme for dynamic crack growth using the extended finite element method *Int. J. Numer. Methods Eng.* **63** 631–59

[87] Réthoré J, Gravouil A and Combescure A 2005 A combined space–time extended finite element method *Int. J. Numer. Methods Eng.* **64** 260–84

[88] Sethian J A *et al* 1999 *Level Set Methods and Fast Marching Methods* (Cambridge: Cambridge University Press)

[89] Shi G-H 1991 Manifold method of material analysis *9th Army Conf. on Applied Mathematics and Computing (US Army Research Office, Minneapolis, MN, USA)*

[90] Simone A, Duarte C A and Van der Giessen E 2006 A generalized finite element method for polycrystals with discontinuous grain boundaries *Int. J. Numer. Methods Eng.* **67** 1122–45

[91] Simone A, Wells G N and Sluys L J 2003 From continuous to discontinuous failure in a gradient-enhanced continuum damage model *Comput. Methods Appl. Mech. Eng.* **192** 4581–607

[92] Song J-H, Areias P M A and Belytschko T 2006 A method for dynamic crack and shear band propagation with phantom nodes *Int. J. Numer. Methods Eng.* **67** 868–93

[93] Stazi F L, Budyn E, Chessa J and Belytschko T 2003 An extended finite element method with higher-order elements for curved cracks *Comput. Mech.* **31** 38–48

[94] Stolarska M, Chopp D L, Moes N and Belytschko T 2001 Modelling crack growth by level sets in the extended finite element method *Int. J. Numer. Methods Eng.* **51** 943–60

[95]   Strouboulis T, Babuška I and Copps K 2000 The design and analysis of the generalized finite element method *Comput. Methods Appl. Mech. Eng.* **181** 43–69

[96]   Strouboulis T, Copps K and Babuška I 2000 The generalized finite element method: an example of its implementation and illustration of its performance *Int. J. Numer. Methods Eng.* **47** 1401–17

[97]   Sukumar N, Chopp D L, Béchet E and Moës N 2008 Three-dimensional non-planar crack growth by a coupled extended finite element and fast marching method *Int. J. Numer. Methods Eng.* **76** 727–48

[98]   Sukumar N, Chopp D L, Moës N and Belytschko T 2001 Modeling holes and inclusions by level sets in the extended finite element method *Comput. Methods Appl. Mech. Eng.* **190** 6183–200

[99]   Sukumar N, Chopp D L and Moran B 2003 Extended finite element method and fast marching method for three-dimensional fatigue crack propagation *Eng. Fract. Mech.* **70** 29–48

[100] Sukumar N, Huang Z Y, Prévost J H and Suo Z 2004 Partition of unity enrichment for bimaterial interface cracks *Int. J. Numer. Methods Eng.* **59** 1075–102

[101] Sukumar N, Moes N, Moran B and Belytschko T 2000 Extended finite element method for three-dimensional crack modelling *Int. J. Numer. Methods Eng.* **48** 1549–70

[102] Sukumar N and Prévost J H 2003 Modeling quasi-static crack growth with the extended finite element method: I. Computer implementation *Int. J. Solids Struct.* **40** 7513–37

[103] Terada K, Asai M and Yamagishi M 2003 Finite cover method for linear and nonlinear analyses of heterogeneous solids *Int. J. Numer. Methods Eng.* **58** 1321–46

[104] Unger J F, Eckardt S and Könke C 2007 Modelling of cohesive crack growth in concrete structures with the extended finite element method *Comput. Methods Appl. Mech. Eng.* **196** 4087–100

[105] van der Giessen E and Needleman A 1995 Discrete dislocation plasticity: a simple planar model *Modelling Simul. Mater. Sci. Eng.* **3** 689–735

[106] Ventura G, Budyn E and Belytschko T 2003 Vector level sets for description of propagating cracks in finite elements *Int. J. Numer. Methods Eng.* **58** 1571–92

[107] Ventura G, Gracie R and Belytschko T 2009 Fast integration and weight function blending in the extended finite element method. *Int. J. Numer. Methods Eng.* **77** 1–29

[108] Ventura G, Moran B and Belytschko T 2005 Dislocations by partition of unity *J. Numer. Methods Eng.* **62** 1463–87

[109] Ventura G 2006 On the elimination of quadrature subcells for discontinuous functions in the eXtended Finite-Element Method *Int. J. Numer. Methods Eng.* **66** 761–95

[110] Waisman H and Belytschko T 2008 Parametric enrichment adaptivity by the extended finite element method *Int. J. Numer. Methods Eng.* **73** 1671–92

[111] Wells G N, Sluys L J and De Borst R 2002 Simulating the propagation of displacement discontinuities in a regularized strain-softening medium *Int. J. Numer. Methods Eng.* **53** 1235–56

[112] Wells G N and Sluys L J 2001 Discontinuous analysis of softening solids under impact loading *Int. J. Numer. Anal. Methods Geomech.* **25** 691–709

[113] Wells G N and Sluys L J 2001 A new method for modelling cohesive cracks using finite elements *Int. J. Numer. Methods Eng.* **50** 2667–82

[114] Williams M L 1961 The bending stress distribution at the base of a stationary crack *J. Appl. Mech.* **28** 78–82

[115] Xiao Q Z, Karihaloo B L and Liu X Y 2007 Incremental-secant modulus iteration scheme and stress recovery for simulating cracking process in quasi-brittle materials using xfem *Int. J. Numer. Methods Eng.* **68** 2606–35

[116] SP Xiao and Belytschko T 2004 A bridging domain method for coupling continua with molecular dynamics *Comput. Methods Appl. Mech. Eng.* **193** 1645–69

[117] Zabaras N, Ganapathysubramanian B and Tan L 2006 Modelling dendritic solidification with melt convection using the extended finite element method *J. Comput. Phys.* **218** 200–27

[118] Zavattieri P D and Espinosa H D 2001 Grain level analysis of crack initiation and propagation in brittle materials *Acta Mater.* **49** 4291–311

[119] Zi G and Belytschko T 2003 New crack-tip elements for XFEM and applications to cohesive cracks *Int. J. Numer. Methods Eng.* **57** 2221–40

[120] Zi G, Song J-H, Budyn E, Lee S H and Belytschko T 2004 A method for growing multiple cracks without remeshing and its application to fatigue crack growth *Modelling Simul. Mater. Sci. Eng.* **12** 901–15

[121] Zohdi T I and Wriggers P 2005 *Introduction to Computational Micromechanics* (Berlin: Springer)